Femtosecond melting and ablation of semiconductors studied with time of flight mass spectroscopy

Andrea Cavalleri,[a] Klaus Sokolowski-Tinten, Joerg Bialkowski, Michaela Schreiner, and Dietrich von der Linde
Institut für Laser und Plasmaphysik, Universität-GHS-Essen, Germany

(Received 1 September 1998; accepted for publication 16 December 1998)

Using time-of-flight mass spectroscopy, we have investigated melting and ablation of gallium arsenide and silicon irradiated by femtosecond pulses. Below the ablation threshold the maximum surface temperature is obtained from the collisionless time-of-flight distributions of evaporated or sublimated particles. At the melting threshold, we estimate a temperature for the silicon surface which is approximately 500 K higher than the equilibrium melting temperature. In the fluence regime where melting is known to be a nonthermal process, we measure maximum surface temperatures in excess of 2500 K for both silicon and gallium arsenide, indicating rapid thermalization after nonthermal melting. At the ablation threshold, we estimated for both materials surface temperatures between 3000 and 4000 K. We observed a clear threshold-like effect in the number of detected particles, indicating the occurrence of a bulk effect. The flow parameters above the ablation threshold are discussed and compared to the different models of collisional expansion. For $F_{abl} < F < 2F_{abl}$, transition from the liquid state to the gas phase occurs through the two-phase regime. For $F > 2F_{abl}$, we find evidence that expansion takes place at temperatures that are higher than the critical temperature. Plasma formation appears only at fluences above 1 J/cm^2 ($F > 5F_{abl}$). © *1999 American Institute of Physics.* [S0021-8979(99)05506-1]

I. INTRODUCTION

Femtosecond laser ablation[1] has recently attracted increasing interest mainly because of its potential in micromachining applications.[2] The mechanisms which eventually lead to material removal are, however, strongly dependent on the specific optical and thermodynamic properties of the solid, laser wavelength, and pulse duration. A complete understanding of the involved phenomena is lacking. If the solid is transparent, for instance, absorption of the optical energy occurs through nonlinear absorption and ablation takes place after optical breakdown and formation of a plasma at the surface.[3,4] On the other hand, in the case of linearly absorbing semiconductors the laser energy is efficiently coupled into the solid and ablation is of thermal nature.[5,6]

Time of flight mass spectroscopy can be applied to experimentally study femtosecond heating, melting, and ablation of a semiconductor. Below the ablation threshold it is possible to estimate the maximum temperature of the molten surface from the velocity distributions of the evaporated and sublimated atoms.[7,8] Above the ablation threshold one can gain some information on the physics of mass flow[9] and on the behavior of the material during the early phase of the expansion.

In a recent letter[10] we have presented time-of-flight (TOF) mass spectroscopy measurements of laser irradiated gallium arsenide, showing that ablation starts from a hot liquid surface and that the TOF distributions are modified by the role of collisions in front of the sample. In the present article, we extend our measurements to silicon and analyze results in more detail.

In Sec. II, we summarize the theoretical frame of our work. We briefly describe ultrafast heating, melting, and ablation in semiconductors (Sec. II A), the regimes of mass flow (Sec. II B) and the appropriate models of TOF distributions (Sec. II C). In Sec. II D we list the problems which are to be addressed with the present experiment. Experimental set-up and procedure are described in Sec. III and the TOF measurements are discussed and compared to optical experiments in Sec. IV. In Sec. V we discuss the results and conclude in Sec. VI.

II. THEORETICAL CONSIDERATIONS

A. Femtosecond heating, melting, and ablation of semiconductors

The fluence range considered in the present article is between 50 and 500 mJ/cm^2, *strictly below the threshold for plasma formation* which is of approximately 1 J/cm^2 (100 fs, 620 nm pulses). The energy is initially absorbed by the carriers of the semiconductor, which undergo interband transitions. Depending on the excitation fluence, several effects can take place after the absorption of the laser pulse. Five fluence intervals can be defined for our experimental conditions:

(a) For the lowest fluence range (below 100 mJ/cm^2 in gallium arsenide and 150 mJ/cm^2 in silicon) the sample does not melt. The hot carriers relax via carrier-carrier and carrier-phonon scattering, eventually recombining

[a]Present address: Department of Chemistry, University of California at San Diego, San Diego California. Electronic mail: axc@chem.ucsd.edu

 © 1999 American Institute of Physics

Downloaded 24 Mar 2009 to 134.100.32.208. Redistribution subject to AIP license or copyright; see http://jap.aip.org/jap/copyright.jsp

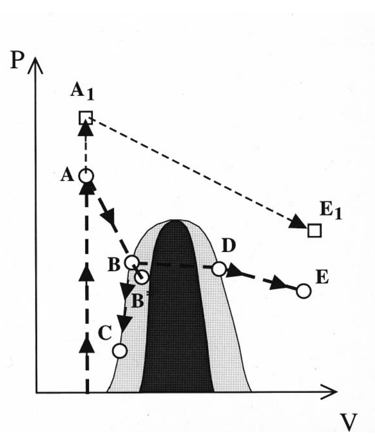

FIG. 1. Schematic van der Waals-like $P-V$ diagram of a material and thermodynamic pathway of ablation.

on a time scale of several picoseconds and transferring most of the absorbed energy to the lattice via delayed Auger heating.[11] Carrier diffusion may be significant on a picosecond time scale.[12]

(b) If the heated lattice reaches temperatures in excess of the melting temperature T_m ($T_m = 1685$ K, $F_m = 150$ mJ/cm^2 in silicon, $T_m = 1513$ K, $F_m = 100$ mJ/cm^2 in gallium arsenide), nucleation of the liquid phase takes place at the surface and a layer of molten material grows into the solid.[13,14] In this regime, the melting process is *strictly thermal*.

(c) At higher fluences melting occurs as an *ultrafast, nonthermal process*.[5,14–18] The excitation of a dense electron-hole plasma occurs, causing destabilization of the lattice, and the semiconductor melts in less than one picosecond.[16,17] In the case of gallium arsenide, a well defined fluence threshold of $F_m^* = 1.5 F_m$ (150 mJ/cm^2) separates the thermal and nonthermal melting regimes.[18]

(d) At laser fluences exceeding the ablation threshold ($F_{abl} = 175$ mJ/cm^2 in gallium arsenide and $F_{abl} = 300$ mJ/cm^2 in silicon) macroscopic amounts of material leave the semiconductor, eventually leaving a crater on the surface.[5]

Figure 1 shows a schematic van der Waals-like $P-V$ diagram. The left and right hand side of the diagram correspond to the liquid and the gas phase of the material, respectively. The darkly shaded area represents the two-phase regime, where the material at equilibrium is composed by an inhomogeneous mixture of the two phases. The two-phase regime is bounded by the binodal curve, which under thermodynamic equilibrium conditions is the boundary between the two-phase regime and homogeneous gas or liquid. However, the material can transiently penetrate into the binodal as a homogeneous metastable phase. The region which in Fig. 1 is lightly shaded, represents the accessible metastable states of the diagram and corresponds to superheated liquid and undercooled gas on the left and right hand side, respectively. The metastable area is delimited by the spinodal (boundary of the dark shaded area), where the elasticity of the material becomes zero and a metastable homogeneous phase becomes unstable.[19] The region which is delimited by the spinodal is not accessible as a homogeneous phase.

A common pathway characterizes the early dynamics after irradiation, for both regimes *c* and *d*. After irradiation, the material melts nonthermally and in about 1 ps it can be regarded as a hot liquid at high pressure (A). Heating and melting of the semiconductor, occurring on a significantly shorter time scale than pressure release, can be regarded as an isochoric process and as a vertical transition in the $P-V$ diagram. If the initial temperature exceeds the critical temperature, the liquid may as well be regarded as a hot fluid which behaves as a gas despite the high density, typical of the liquid phase. The pressure is then released through mechanical expansion of the material which undergoes adiabatic cooling while remaining in the liquid state ($A \rightarrow B$). Mechanical expansion occurs at a speed which is limited by the speed of sound in the liquid and therefore within several picoseconds. Expansion takes place until the binodal is reached and the material enters the two-phase regime.[6] Crossing of the binodal as a homogeneous liquid corresponds to the formation of a superheated state (B^*), which tends to homogeneously nucleate the gas phase (gas bubbles) at a rate which increases with the degree of superheating of the material. It is to be stressed that homogeneous boiling (phase explosion) occurs over the whole liquid layer and not only at the surface as heterogeneous boiling.[20] However, because of heat diffusion, the liquid tends to cool along the binodal and to remain in the liquid state ($B \rightarrow C$). Competition between nucleation of the gas phase and cooling most likely determines whether ablation takes place or not. Since the rate of bubble formation is a very steep function of the amount of superheating[20,21] the ablation threshold observed in femtosecond irradiation of semiconductors is very sharp.[5,6]

Whenever ablation takes place, homogeneous nucleation of gas bubbles rapidly transforms the liquid into a mixture of coexisting phases, eventually creating a system of droplets immersed into a gas. Progressive evaporation follows the path $B \rightarrow D$. After several nanoseconds,[5,6] the material transforms into a gas, which can either be composed of single atoms or of several molecular species ($D \rightarrow E$).

A fifth fluence regime is represented by the $A_1 \rightarrow E_1$ pathway. If the initial pulse is energetic enough, the material is heated to a point where adiabatic expansion can take place without entering the two-phase regime. Molecular dynamics simulations confirm this picture.[22] In this case, expansion proceeds above the critical isotherm, no nucleation of the gas phase is required and the material behaves in first approximation as an ideal gas.

B. Regimes of mass flow

(a) As described in Sec. II A this fluence regime corresponds to heating of the solid phase without melting. Sublimation from the solid occurs at the surface and detachment of single atoms[23] and/or clusters[24] takes place.

(b) Superheating of the solid and melting at the surface takes place after deposition of the laser energy. Sublimation from the superheated solid surface and subse-

Downloaded 24 Mar 2009 to 134.100.32.208. Redistribution subject to AIP license or copyright; see http://jap.aip.org/jap/copyright.jsp

quent evaporation from the liquid contribute to the flow of atoms and clusters. Whether most of the particles leave the surface in the solid or liquid phase is a matter of melting time, surface temperature evolution $T_s(t)$ and of sublimation and evaporation probabilities.

(c) The material melts nonthermally in a subpicosecond time scale and evaporation from the rapidly formed liquid phase is likely to be the only relevant effect. Strictly speaking, evaporation at equilibrium can only take place at point (B) or (B^*) of the $P-V$ diagram shown in Fig. 1, where the gas phase can be accessed. It is, however, possible that some particles leave the surface nonthermally when the material has not yet reached the binodal. Sublimation and evaporation of atoms and clusters are processes of similar nature, in this article they are generally referred to as ''desorption of particles'' whenever further specification is not necessary. Assuming thermodynamic equilibrium, the flux of particles as a function of the surface temperature can be quantitatively described by[23]

$$J(T)=\frac{p_0}{\sqrt{2\pi m k_b T_s}}\exp[-(E_A/k_bT_s)]. \tag{1}$$

In Eq. (1), p_0 is a constant, m is the mass of the desorbed particle, k_b is the Boltzman constant, and E_A is the relevant activation energy. Below the ablation threshold less than a monolayer leaves the surface and mass flow is collisionless.

In this case, mass flow proceeds as initial expansion of a liquid followed by progressive creation of gas bubbles in the bulk of the expanding layer. Eventual formation of a homogeneous dense gas takes place after the phase transition and further dilution brings the ablated material into the collisionless flow regime. The evolution of density, pressure, temperature, and flow velocity is, in this case, a complicated function of both space and time and to our knowledge no complete solution of the flow problem exists, as the details of the equation of state are to be taken into account.[6,25]

In the case of flow above the critical point, the material undergoes expansion behaving in first approximation as an ideal gas. The simplest approach consists in treating the flow as fully continuum-like, using the formalism of a centered rarefaction wave.[26] The particles expand with a flow velocity which is a linear function of the position in the profile. Velocity of the particles varies from 0 to $v_{\max}=2c_0/(\gamma-1)$, where c_0 is the initial sound velocity in the unexpanded reservoir and $\gamma=C_p/C_v$ is the adiabatic coefficient in the gas. In the case of an ideal gas, γ=5/3 and $c_0=(\gamma k_b T_r/m)^{1/2}$, where T_r is the temperature in the reservoir and m is the mass of the particle, which gives $v_{\max}=3c_0 =(15k_bT_r/m)^{1/2}$. This picture applies to the early phase of the supercritical flow. However, in an expansion into vacuum the rarefaction wave has always an underdense tail in which the continuum picture is no longer valid and ballistic flow takes place. Thus, the solely hydrodynamic description of the expansion is, strictly speaking, incorrect. Generally, the correct approach to the problem consists in the numerical solution of the kinetic equation of the gas over a wide enough time interval.[27] The ''Knudsen layer'' model is appropriate in the intermediate density regime, where collisions achieve thermalization into the gas, but the conditions for continuum-like flow are not met. Expansion of a dense gas from a reservoir is to be described schematically as follows: after leaving the surface the particles thermalize with one another in a region of space known as the Knudsen layer, followed by the so called ''unsteady adiabatic expansion'' layer which among further rarefaction transforms into a free flow region.[28] In this case, one cannot describe the velocity of the particles as an analytic function of space and time.

A special case is the formation of a Knudsen layer *without* unsteady adiabatic expansion, which describes collisional flow at low densities. In this case, after evaporation the gas achieves thermalization in the Knudsen layer and it expands further directly by free flow. However, in most practical cases such a description is an oversimplification of the problem and unsteady adiabatic expansion has to be taken into account after thermalization in the Knudsen layer.

C. The time of flight problem

The regimes $(a)-(c)$ are characterized by the absence of interaction between the released atoms/clusters after desorption. The velocity distribution of the particles in front of the sample is a so called ''half range Maxwellian''. The released particles posses only positive velocities because no back scattering event occurs during the flight. If the TOF signal is measured by a spectrometer plus an ionizer, the distribution of the desorbed particles can be written as

$$f(t)=A/t^4\exp[-(m/2k_bT_0)L^2/t^2], \tag{2}$$

where L stands for the distance travelled before ionization and T_0 represents the characteristic temperature of the distribution. In the case of femtosecond laser irradiation of semiconductors, this model can be applied up to the ablation threshold.[10] The TOF distributions of regimes $(a)-(c)$ are fitted with Eq. (1) and the obtained temperature T_0 is considered a good approximation of the maximum surface temperature T_s because the flux of desorbed particles depends exponentially on the surface temperature. Let us discuss such assumptions in detail.

The surface temperature of the irradiated sample is a function of both time and space, due to heating and cooling of the sample and to the gaussian spatial distribution of the laser beam. Given the spatial and temporal dependence of the surface temperature ($T_s[x,y,t]$, where x,y are the spatial coordinates on the surface and t the temporal coordinate), the expected velocity distribution $g'(v)$ arises from integration of $g(v,T)$ weighted through the flux expression of Eq. (1),

$$g'(v)=\int_t\int_x\int_y J(T_s[x,y,t])g(v,T_s[x,y,t])dxdydt. \tag{3}$$

The obtained integrated velocity distribution $g'(v)$ can be fitted with Eq. (2) whenever the activation energy of Eq. (1) is above 0.3 eV.[29] T_0 is, in general, an underestimation of T_s. The error can be calculated if E_A and $T_s[x,y,t]$ are known and it increases at high temperatures and for low activation energies.

Downloaded 24 Mar 2009 to 134.100.32.208. Redistribution subject to AIP license or copyright; see http://jap.aip.org/jap/copyright.jsp

In regimes (*d*) and (*e*) the time of flight problem must take collisions into account. As already noted, the velocity distribution of gallium atoms can no longer be described by Eq. (3) because a nonzero drifting velocity develops due to interaction in front of the sample. The new TOF distribution, known as full range Maxwellian, is therefore to be described by

$$f(t)=A/t^4 \exp[-(m/2k_bT_d)(L-v_dt)^2/t^2], \quad (4)$$

where T_d and v_d are temperature and drift velocity of the particle distribution, respectively.

In the case of the formation of a Knudsen layer without unsteady adiabatic expansion, one can give some physical significance to the fitted parameters. T_d and v_d give, in this case, the temperature and the most probable velocity at the outer border of the Knudsen layer, which acts as new boundary condition for the free flow problem. Under such conditions, the most probable velocity attained by the particles beyond the Knudsen layer lies within 2% of the sound velocity in the expanding gas.[30] The temperature T_d is, in this case, equal to approximately 2/3 of the surface temperature before expansion.

If unsteady adiabatic expansion *does* take place after thermalization, the drift velocity tends to increase further and to slightly exceed the velocity of sound in the Knudsen layer. However, the presence of unsteady adiabatic expansion does not significantly perturb the drift.[30]

If one assumes that the expansion process is fully continuum-like, T_d *does not* represent a physical temperature. Instead, it provides only a flow parameter as different velocity components of the centered rarefaction wave correspond to different temperatures. Similarly, the drift velocity v_d does not represent the average flow velocity. Temperature and flow velocity distributions of the expanding gas can only be found by solving the hydrodynamic equations.[31] The application of a hydrodynamic model for the time of flight problem requires that the detector be at finite distance from the sample, that is to say no more than a few hundred microns form the semiconductor surface. Since in our experimental conditions the detector is effectively at infinite distance from the sample (several tens of centimeters), no solely continuum picture can be applied to the TOF problem as this would formally imply zero density and temperature at the detector.[26]

D. Open questions

The present experiments are meant to address the following questions: First, the law of growth in the number of neutrals with laser fluence, as well as neutral to ions ratio in the ablation products are an interesting information to determine the onset of plasma formation. Second, in regime (*c*), the nonthermally molten surface is known to rapidly reach a conventional thermodynamic state in a few hundred femtoseconds after irradiation. However, no experimental data exist on the temperature of a nonthermally molten semiconductor. Third, ablation is known to occur by progressive dilution as an inhomogeneous phase through the coexistence regime. The measured temperature in regime (*c*) is related to the conditions of the surface of the mechanically relaxed liquid at the binodal. The temperature at threshold must be lower than the critical temperature of the material to confirm our view of close to threshold thermal ablation. Fourth, analysis of the fitted flow parameters above the ablation threshold and comparison with optical experiments is required to complete the explanation of thermal ablation in regimes (*d*) and (*e*).

III. EXPERIMENTS

Experiments were performed on surfaces of GaAs[100], Si[111], and Si [100] which where placed in Ultra High Vacuum at 10^{-10} Torr and irradiated with femtosecond visible pulses of characteristic energy densities between 50 to about 500 mJ/cm^2. The samples where illuminated at an angle of incidence of 45° with *p*-polarized laser radiation. Pulses of 100–120 fs at 620 nm and up to 4 mJ energy were provided by a colliding pulse mode-locked dye laser followed by a three stage Nd:(YAG) (yttrium-aluminum-garnet) pumped dye amplifier system, operating at 10 Hz repetition rate. Single pulses were selected from the 10 Hz pulse train by suitably switching a computer controlled mechanical shutter. The samples were translated *in vacuo* after single shot irradiation, in order to provide a fresh surface area for each laser pulse. The laser pulse energy was continuously varied by means of rotating a half wave plate in front of a polarizer and measured with calibrated fotodiodes. After every experiment a series of craters at several pulse energies were produced on the sample in vacuum. By means of plotting the measured area of the craters as a function of the logarithm of the pulse energy, the absolute calibration of laser fluence, ablation threshold, spatial quality of the laser on the sample, as well as beam parameter were carefully controlled in every measurement.[14] The experiments where always carried out under conditions of a spatially gaussian laser pulse.

TOF distributions of neutral particles leaving the surfaces were measured using a quadrupole mass spectrometer (QMS). Desorbed neutrals were ionized at the entrance of the QMS by means of an electron beam and detected after mass selection. The QMS used in our experiment was capable of detecting up to mass-to-charge ratios of 300. Single shot distributions were read by a digital oscilloscope and stored by a computer which provided the average distributions for each fluence interval. At the lowest irradiation fluences of 50–100 mJ/cm^2 less than one particle per shot was detected, requiring typical averages over up to 10^4 single shot experiments. Figure 2 shows examples of average TOF distributions of silicon atoms obtained from silicon surfaces for three different fluence ranges: below the melting threshold, between the melting and the ablation threshold, and above the ablation threshold. They resemble maxwellian distributions and the average time of flight progressively decreases with increasing fluence.

IV. EXPERIMENTAL RESULTS AND ANALYSIS

A. Total number of detected particles

Using the procedure described above, TOF distributions where obtained and sorted as a function of the laser fluence.

Downloaded 24 Mar 2009 to 134.100.32.208. Redistribution subject to AIP license or copyright; see http://jap.aip.org/jap/copyright.jsp

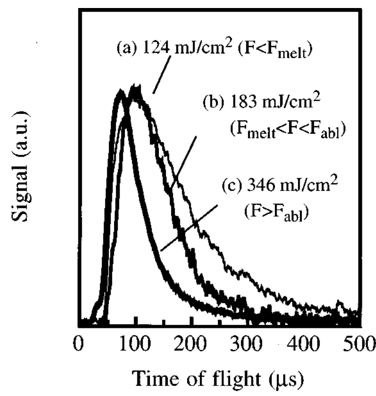

FIG. 2. Examples of TOF distributions from silicon surfaces for three different fluences. The three curves represent results: below the melting threshold, between the melting and the ablation threshold, and above the ablation threshold.

The total number of neutral particles at a given fluence can be obtained by integrating in time $S(t)/t$, where $S(t)$ is the time of flight signal and t the time variable. The necessity of dividing the detected signal by the time variable to obtain the number of ablated particles comes from the inverse dependence of the detection efficiency on the velocity in the ionization volume. Figure 3 shows the number of detected gallium (GaAs) and silicon atoms as a function of the laser fluence normalized to the respective ablation thresholds. The behavior of the total number of desorbed particles is clearly depending on whether the normalized fluence is smaller or bigger than 1.

For fluences below the ablation threshold ($F/F_{th}<1$), where the detachment of particles is dominated by desorption (evaporation/sublimation), the law of growth is clearly dependent on the type of material. The number of detected silicon particles is lower than that of gallium for a given normalized fluence, growing steeply as the ablation threshold is approached. Note that the total number of gallium particles experiences an abrupt increase across the fluence corresponding to the ablation threshold. For $F/F_{th}>1$, the law of growth seems to become very similar for the two materials. The total number of detected ions (Si_1^+,Ga_1^+) is at least one order of magnitude below that of the detected neutrals, starting to increase only above about 1 J/cm^2, where ionization is significant.

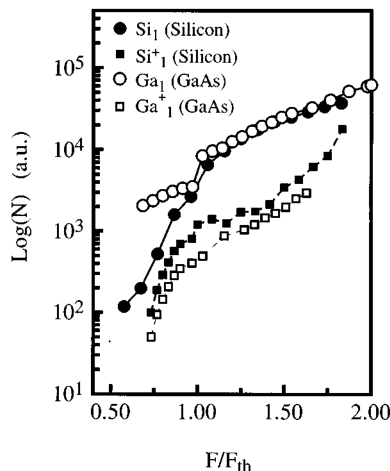

FIG. 3. Total number of detected neutrals and ions as a function of laser fluence normalized to the respective ablation thresholds. Full dots: Silicon neutrals. Full squares: Silicon ions, ablation threshold 300 mJ/cm^2. Empty circles: Gallium (GaAs). Empty squares: Gallium (GaAs), ablation threshold 175 mJ/cm^2.

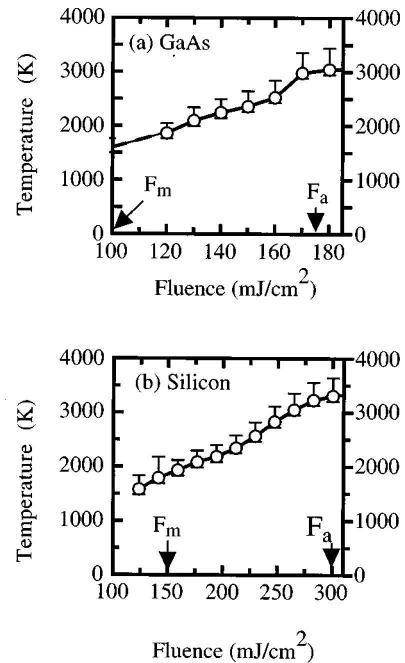

FIG. 4. Fitted surface temperatures of (a) gallium arsenide and (b) silicon. The error bars represent systematic errors and underestimation due to spatial and temporal integration effects.

In the case of gallium arsenide, we observe only monoatomic gallium, whereas molecular clusters are observed for arsenic. In the case of silicon, we generally detect molecular species composed by up to 6 atoms. The absolute numbers of the detected molecules decreases with the size of the molecule. Below the ablation threshold the Si_1/Si_2 ratio is of the order of 100. The existence of clusters up to Si_6 among the desorption products has been reported to occur from heated silicon surfaces, the relative amounts being related to the different activation energies of the various molecular desorption processes.[23] The ratio between single atoms and higher order molecular species is, however, a decreasing function of the fluence, for Si_1/Si_2 it reaches 28 at F_{th} and 8 at $1.5\,F_{th}$.

B. Surface temperature measurements for $F<F_{abl}$

The distribution of both gallium and silicon can be fitted very well with half range maxwellians, where the only free parameter is the temperature T_0 of Eq. (2). Figure 4 shows the results of our fits for both gallium arsenide (gallium) and silicon atoms. In the case of silicon, the distributions of higher order molecules tend to give the same surface temperatures as those of Si_1, although their low number causes a rather poor signal to noise ratio. No difference was found between the measurements on Si[111] and Si[100] surfaces.

We observe a monotonically increasing temperature with increasing laser fluence. Close to the ablation threshold, the temperature tends to stabilize on a plateau, below the critical

Downloaded 24 Mar 2009 to 134.100.32.208. Redistribution subject to AIP license or copyright; see http://jap.aip.org/jap/copyright.jsp

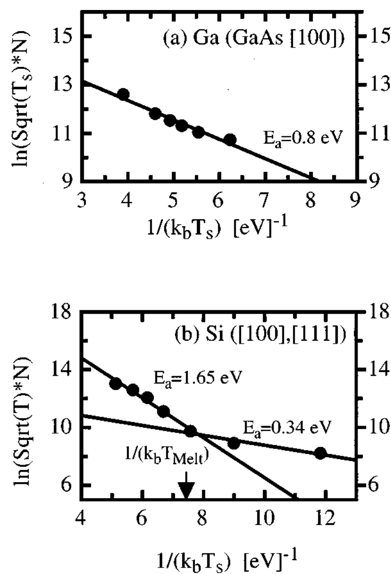

FIG. 5. Arrhenius plot for (a) Gallium from GaAs[100] and (b) Silicon atoms from Si[100] and Si[111].

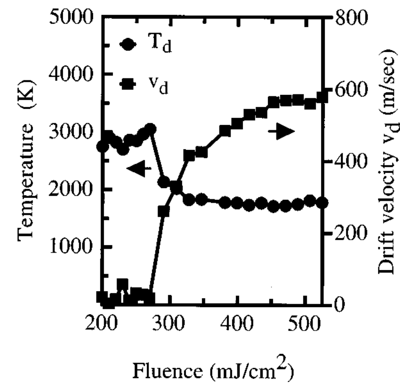

FIG. 6. Temperature and drift velocity of gallium particles detected from gallium arsenide at fluences above the ablation threshold.

temperature (in silicon $T_c \approx 5160\,\mathrm{K}$).[32] The systematic uncertainty on the measured temperature is approximately ± 100 K.

The underestimation of the maximum surface temperature due to spatial and temporal averaging is calculated as follows. The relevant value of the activation energy E_A is estimated from Eq. (1) by means of substituting the fitted temperature as surface temperature. The logarithm of the total number of detected particles multiplied by $\sqrt{T_0}$ shows a linear dependence on $1/k_b T_0$, as can be inferred from Eq. (1). The slope gives the activation energy (see Fig. 5). In the fluence interval between the melting and the ablation threshold, the plot is linear and the activation energies are 0.8 eV for gallium and 1.65 eV for silicon. In the case of silicon, our measurements where extended to fluences which are lower than the melting threshold [regime (*a*)]. Below the melting temperature, we observe a change in slope and a lower activation energy of 0.34 eV is measured for sublimation from the excited solid surface. The initial spatial distribution of the temperature can be evaluated starting from the gaussian beam parameter measured on the sample,[33] whereas the temporal evolution has been calculated by numerically solving the heat flow equation for the physical conditions of regime (*b*).[18,34] Combining the temporal and spatial behavior with Eq. (3), we calculate the effective velocity distribution $g'(v)$ from which we obtain an effective time of flight signal $f'(t)$. By fitting $f'(t)$ with $f(t)$ from Eq. (2), we obtain T_0, which we compare with the calculated surface temperature $T_s(t)$.

The maximum underestimation of the temperature of the surface is included in the error bars of Fig. 4. Below the melting threshold, the fitted temperature underestimates of the maximum surface of *solid* silicon by 250–500 K. Above the melting threshold, the effective temperatures extracted from $f'(t)$ are found to be slightly below the maximum temperature of the *liquid* surface, that is to say after the phase transition has taken place a few picoseconds after irradiation. For laser fluences corresponding to fluence regime (*c*), no detailed calculations are at our disposal since the model described in Ref. 34 is strictly valid under thermal melting conditions. However, in the fluence regime (*c*), where the phase transition occurs even faster than in regime (*b*), the fitted temperature represents *a fortiori* the maximum temperature of the liquid after rapid nonthermal melting has taken place.

C. Measurements above the ablation threshold

As shown in Ref. 10, gallium TOF can be successfully fitted using Eq. (4). For $F > F_{\mathrm{th}}$, the fitted parameters (T_d and v_d) are shown in Fig. 6. Above $1.5\,F_{\mathrm{th}}$ (250 mJ/cm^2), the measured temperature is observed to drop towards a plateau at approximately 1800 K, which is already reached for fluences below $2\,F_{\mathrm{th}}$ (about 300 mJ/cm^2). The drift velocity increases towards 600 m/s, although it stabilizes only at higher fluences than those at which the temperature plateau is reached (above 450 mJ/cm^2, approximately $2.5\,F_{\mathrm{th}}$.

Concerning the expansion of arsenic particles, the detected species range from As_1 to As_4 ($m/e = 300$ amu), which is the limit of our QMS. The total number of detected molecules was comparable with that of the monomers, and the distributions were generally non-Maxwellians, in contrast to what observed below the ablation threshold.

In the case of Silicon, instead, the distributions where Maxwellians for both Si_1 and Si_2. The distributions of the other molecular clusters (Si_3–Si_6) were generally non-Maxwellian. Most likely, our Si_n distributions are affected by crack products of larger molecules produced in the ionization volume of the QMS.

D. Optical measurements

Figure 7 shows snapshots of the silicon and gallium arsenide surfaces taken with femtosecond time resolved microscopy.[35] These pictures have been obtained by using a delayed probe pulse as illumination of an optical microscope. Because of the gaussian spatial profile of the pump pulse, different positions on the picture correspond to different local pump fluences.[5,6] The pictures taken on silicon at -100 fs and 1 ps time delay show that the initially semiconducting solid surface melts in about 1 ps and becomes a metallic

Downloaded 24 Mar 2009 to 134.100.32.208. Redistribution subject to AIP license or copyright; see http://jap.aip.org/jap/copyright.jsp

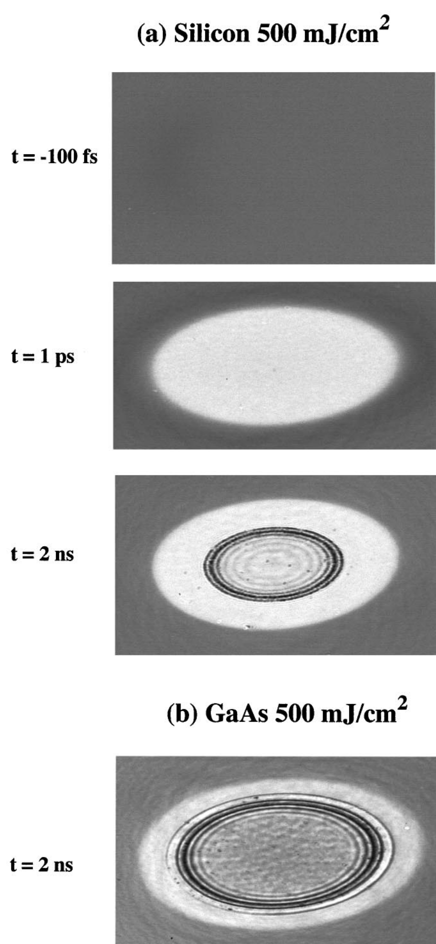

FIG. 7. Snapshot of the vaporization process taken on a silicon and gallium arsenide surfaces after irradiation with a 500 mJ/cm^2 pulse.

liquid, as discussed in Sec. II A. Pictures at 2 ns time delay represent the behavior, of the material during expansion. A bright ring which has exactly the reflectivity of the liquid is visible in the outermost region of the originally molten area. This region is irradiated with a fluence exceeding the melting threshold but below that for ablation and is, at this time delay, in the liquid state [regimes (b) and (c)]. Above the independently measured ablation threshold Newton rings arise from thin film interference in the layer of ablated material.[6] The ablated material consists of an inhomogeneous system of liquid droplets (metallic) immersed in a dense gas $(n \approx 1)$, where the low sound velocity of the two phase regime[36] is responsible for the formation of a steep front towards vacuum[6,25] [regime (d)]. At later time delays (not shown here), the material vaporizes completely and the rings disappear. Micrographs taken virtually at infinite time delays (several seconds after irradiation) show the formation of a crater exactly on the same surface where the transient Newton rings have been observed.

In gallium arsenide, when the local laser fluence crosses $F = 315\,\mathrm{mJ/cm}^2\,(F/F_{\mathrm{abl}} = 1.8)$ the ring-like structure never appears, indicating that the front towards vacuum ceases to be steep. In silicon, we observe similar disappearance of the rings at about $F = 450\,\mathrm{mJ/cm}^2\,(F/F_{\mathrm{abl}})$. Such effect occurs because the expanding materials are no longer in the two-phase regime for fluences which exceed this second threshold. Rather, the material behaves as in regime(e), as described in Sec. II A.

V. DISCUSSION

The number of desorbed neutrals in gallium arsenide nearly triples for a fluence variation of $\pm 3\%$, indicating the transition to a bulk effect upon the occurrence of ablation. Post mortem analysis of the craters left on the GaAs surface shows that craters as deep as 20 nm and with steep lateral walls are created also slightly above the threshold. In silicon, we observe a similar effect.

The low number of detected ions shows that the threshold for plasma formation has not been reached, in accordance with what concluded from optical experiments. The ionisation probability in the QMS of the neutrals being less than 1%, it must be concluded that the number of ions which leave the surface under our experimental conditions is more than three order of magnitudes below that of the neutrals.

Let us now discuss the experiments concerning the surface temperature below the ablation threshold for the fluence regimes $(a)-(c)$:

(a) In both gallium arsenide and silicon, the estimated surface temperatures seem to slightly exceed the respective equilibrium melting temperature at the corresponding fluence threshold (independently determined). At the melting threshold, the measured silicon surface temperature is of about 1850 K, with underestimation of the order of 350 K. The estimated activation energy of the solid for $T < T_m$ is of 0.34 eV, clearly below what is known to be the activation energy for desorption of single atoms, which is of about 4.6 eV.[33] This discrepancy may be caused by some superheating of the solid surface.[8] The surface of a solid which is in a metastable state would be most likely unstable, resulting in an enhanced detachment of atoms. Another possibility would be the occurrence of a nonthermal ablation process, similar to photophysical ablation of polymers.[37] However, no definite statement can be made on the basis of our data.

(b) Above the melting threshold, we observe indeed a change in the surface activation energy in silicon, indicating that the observed particles are evaporated from a liquid surface, as concluded after the analysis discussed in Sec. II C.

(c) At fluences at which melting is nonthermal in nature, we observe no significant discontinuity in the maximum temperature of the surface. Moreover, the activation energy of the surface remains the same as that observed at lower temperatures, as indicated from the linearity of the plots of Fig. 5 across both fluence regimes. This result shows that after nonthermal melting, semiconductors thermalize rapidly as hot liquids in the normal thermodynamic state.[9] No indication of a significant nonthermal contribution to the desorption process can be detected. The temperature of the surface at the ablation threshold is, for both materials, between 3000 and 4000 K. The case of silicon is particularly

Downloaded 24 Mar 2009 to 134.100.32.208. Redistribution subject to AIP license or copyright; see http://jap.aip.org/jap/copyright.jsp

instructive, because the surface temperature is significantly lower than the estimated $T_c = 5160\,\mathrm{K}$, indicating that expansion is indeed undercritical.

(d) Slightly above the ablation threshold no drift velocity is necessary to fit our data, and the distributions are apparently half range. However, slightly above threshold neither of the two TOF models gives reliable results, since the observed distribution represents a spatial average over the central area where ablation occurs, and outer areas below threshold where particle emission is due to evaporation. Figure 3 shows that just above the ablation threshold the total number of particles amounts to about 2–3 times that measured below, suggesting that ablation and desorption contribute with comparable amounts to the measured signal. When the fluence reaches about 1.5 F_{abl}, we estimate that more than 90% of the total number of detected particles are due to ablation. Therefore, we assume that in this case Eq. (4) provides a reliable model. The measured T_d drops and stabilizes on a plateau at 1800 K above a fluence of approximately 300 mJ/cm^2 ($1.7\,F_{\mathrm{abl}}$) where the detected atoms are almost solely released from the regions of the surface undergoing ablation. At this point the fitted drift velocity is approximately 350 m/s, still increasing with fluence. The measured drift velocity is not compatible with what is expected for collisional flow of a homogeneous gas. As explained in Sec. II C, whenever a full Knudsen layer is formed the most probable velocity coincides approximately with the speed of sound in the gas. Assuming ideal gas behavior, for $T_d = 1800\,\mathrm{K}$ and $\gamma = 5/3$, $v_d = (\gamma k_b T_r/m)^{1/2} = 600\,\mathrm{m/s}$. A drift velocity below 500 m/s cannot be explained for a gas ($\gamma > 1$). We consider the unusually low drift velocity as a further indication that the early phase of the expansion takes place through the two phase regime and that an inhomogeneous phase with low sound velocity forms in front of the sample.

(e) The drift velocity stabilizes only above 450 mJ/cm^2 ($2.6\,F_{\mathrm{abl}}$) on a value of approximately 600 m/s, which coincides with the sound velocity in an ideal gas ($\gamma = 5/3$) composed of gallium atoms (69 amu) at 1800 K. This measurement is consistent with: (1) the formation of a full Knudsen layer in front of the sample, probably followed by unsteady adiabatic expansion, and (2) the expansion as an ideal gas above $2.5\,F_{\mathrm{abl}}$, indicating that indeed the material does not enter the two-phase regime and undergoes supercritical ablation ($A_1 -> E_1$).

In this respect, let us compare the data of the TOF measurements to those of the optical experiments in the case of gallium arsenide. The rings disappear when the *local* fluence F exceeds $1.8\,F_{\mathrm{abl}}$. The time of flight parameters show, as well, an ideal gas behavior when the *average* fluence exceeds $2.5\,F_{\mathrm{abl}}$, where the majority of the released particles indeed undergoes supercritical expansion. The two observations are in reasonable agreement.

Optical data on silicon suggest a similar behavior, disappearance of the the rings is observed at about $2.5\,F_{\mathrm{abl}}$.

VI. CONCLUSIONS

In conclusion, the problem of femtosecond-laser melting and ablation in covalently bonded semiconductors has been studied with TOF mass spectroscopy. We analyze limits and applicability of TOF mass spectroscopy to temperature measurements in surfaces excited below the ablation threshold.

For silicon, we estimate a surface temperature at the melting threshold which is in excess of the equilibrium melting temperature by about 500 K. The possible sources of such the effect, ranging from superheating of the solid phase to nonthermally assisted ablation are discussed.

Above the melting threshold, the semiconductor melts either thermally or nonthermally. The surface temperature thermalizes at high temperature *independently* from the thermal or nonthermal nature of the phase transition. The activation energy of the molten silicon and gallium arsenide surfaces are measured and they do not show any discontinuity across the range where melting becomes nonthermal. At the ablation threshold, the surface is shown to have a surface temperature which is below the critical temperature.

Above the ablation threshold, dilution of the hot surface results in a transient inhomogeneous phase composed by gas and liquid droplets, as indicated by the low drift velocities measured for particles which undergo ablation for $1.5 < F < 1.8\,F_{\mathrm{abl}}$. At higher fluences ($F > 1.8\,F_{\mathrm{abl}}$) in gallium arsenide adiabatic expansion can take place in a supercritical, fluid state ($\gamma = 5/3$). Plasma formation occurs only at fluences above 1 J/cm^2 ($F > 5\,F_{\mathrm{abl}}$).

More work is required to understand the origin and the expansion dynamics of the bigger molecular species which are found in the ablation debris of silicon.

ACKNOWLEDGMENTS

A. Cavalleri acknowledges financial support from the *European Community* within the program *Human Capital and Mobility*. K. Sokoloavski-Tinten gratefully acknowledges support from the *Flughafen Frankfurt Main* foundation. The authors are also indebted to Vasan Venugopalan from the University of California at Irvine and Barbara Garrison of Pennsylvania State University for providing important literature during the work.

[1] C. Momma, B. N. Chichkov, S. Nolte, F. von Alvensleben, A. Tünnermann, H. Welling, and B. Wellegehausen, Comments Plasma Phys. Control. Fusion **129**, 134 (1996); S. Nolte, C. Momma, H. Jacobs, A. Tünnermann, B. N. Chickov, B. Wellegehausen, and H. Wellig, J. Opt. Soc. Am. B **14**, 2716 (1997).
[2] X. Liu, D. Du, and G. Mourou, IEEE J. Quantum Electron. **33**, 1706 (1997).
[3] D. von der Linde and H. Schüler, J. Opt. Soc. Am. B **13**, 216 (1995).
[4] D. Du, X. Liu, G. Korn, J. Squier, and G. Morou, Appl. Phys. Lett. **64**, 3071 (1994); W. Kautek, J. Krüger, M. Lenzner, S. Sartania, Ch. Spielmann, and F. Krausz, *ibid.* **69**, 3146 (1996); M. Lenzer, J. Krüger, S. Sartania, Z. Cheng, Ch. Spielmann, G. Morou, W. Kautec, and F. Krausz, Phys. Rev. Lett. **80**, 4076 (1998).
[5] D. von der Linde, K. Sokolowski-Tinten, and J. Bialkowski, Appl. Surf. Sci. **109/110**, 1 (1997); K. Sokolowski-Tinten, J. Bialkowski, A. Cavalleri, and D. von der Linde, *ibid.* **127/129**, 755 (1998).

Downloaded 24 Mar 2009 to 134.100.32.208. Redistribution subject to AIP license or copyright; see http://jap.aip.org/jap/copyright.jsp

[6] K. Sokolowski-Tinten, J. Bialkowski, A. Cavalleri, D. von der Linde, J. Meyer-ter-Vehn, A. Oparin, and S. I. Anisimov, Phys. Rev. Lett. **81**, 224 (1998).
[7] B. Stritzker, A. Pospiesczyk, and J. A. Tagle, Phys. Rev. Lett. **47**, 356 (1981).
[8] N. Fabricius, P. Hermes, D. von der Linde, A. Pospiesczyk, and B. Stritzker, Solid State Commun. **58**, 239 (1986); P. Hermes, B. Danielzik, D. von der Linde, J. Kuhl, J. Heppner, B. Stritzker, and A. Pospieszczyk, Appl. Phys. A: Solids Surf. **36**, 1 (1986).
[9] R. Kelly and R. W. Dreyfus, Surf. Sci. **198**, 263 (1988); R. Kelly, A. Miotello, B. Braren, A. Gupta, and K. Casey, Nucl. Instrum. Methods Phys. Res. B **65**, 187 (1992).
[10] A. Cavalleri, K. Sokolowski-Tinten, J. Bialkowski, and D. von der Linde, Appl. Phys. Lett. **72**, 2385 (1998).
[11] M. C. Downer, and C. V. Shank, Phys. Rev. Lett. **56**, 761 (1986).
[12] C. V. Shank, R. Yen, and C. Hirlimann, Phys. Rev. Lett. **51**, 900 (1983).
[13] F. Spaepen and D. Turnbull, in *Laser Annealing of Semiconductors*, edited by J. M. Poate and J. W. Mayer (Academic, New York, 1982).
[14] K. Sokolowski-Tinten, H. Schulz, J. Bialkowski, and D. von der Linde, Appl. Phys. A: Solids Surf. **53**, 227 (1991); K. Sokolowski-Tinten, J. Bialkowski, and D. von der Linde, Phys. Rev. B **51**, 14186 (1995).
[15] P. Saeta, J. K. Wang, Y. Siegal, N. Bloembergen, and E. Mazur, Phys. Rev. Lett. **67**, 1023 (1991).
[16] P. Stampfli and K. H. Benneman, Phys. Rev. B **49**, 7299 (1994).
[17] P. L. Silvestrelli, A. Alavi, M. Parrinello, and D. Frenkel, Phys. Rev. Lett. **77**, 3149 (1996).
[18] K. Sokolowski-Tinten, J. Bialkowski, M. Boing, A. Cavalleri, and D. von der Linde, Phys. Rev. B **58**, 11805 (1998).
[19] V. P. Skripov, J. Non-Equilib. Thermodyn. **17**, 193 (1992).
[20] A. Petrolongo, A. Miotello, and R. Kelly, Phys. Rev. E **50**, 4716 (1994); R. Kelly and A. Miotello, Appl. Phys. Lett. **67**, 3535 (1995).
[21] M. M. Martinyuk, Russ. J. Phys. Chem. **57**, 810 (1983).
[22] S. I. Anisimov (private communication).
[23] G. M. Rosenblatt, in *Treatise on Solid State Chemistry*, Surf (I) Vol. 6A, edited by N. B. Hannay (Plenum, New York, 1976).
[24] H. Tanaka and T. Kanayama, J. Vac. Sci. Technol. B **15**, 1613 (1997).
[25] S. I. Anisimov, N. A. Inogamov, A. M. Oparin, B. Rethfeld, T. Yabe, M. Ogawa, and V. Fortov, in *High Power Laser Ablation*, edited by C. R. Phipps, Proc. SPIE 3343 (in print).
[26] Y. B. Zeldovic and Y. B. Raizer, *Physics of Shock Waves and High Temperature Hydrodynamic Phenomena* (Academic, New York, 1996), Vol. I.
[27] S. I. Anisimov and A. K. Rakhmatulina, Sov. Phys. JETP **37**, 441 (1973).
[28] R. Kelly and R. W. Dreyfus, Nucl. Instrum. Methods Phys. Res. B **32**, 341 (1988).
[29] B. Danielzyk, Ph.D. thesis, University of Essen, 1988.
[30] R. Kelly and R. W. Dreyfus, Surf. Sci. **198**, 263 (1988), and references therein.
[31] S. I. Anisimov, B. S. Luk'yanchuk, and A. Luches, JETP **81**, 129 (1995).
[32] C. L. Yaws, L. L. Dickens, R. Lutwack, and G. Hsu, Solid State Technol. **24**, 87 (1981).
[33] J. M. Liu, Opt. Lett. **7**, 196 (1982).
[34] D. von der Linde, N. Fabricius, B. Danielzyk, and T. Bonkhofer, in *Beam-Solid Interactions and Transient Processes, 1986*, edited by M. O. Thompson, S. T. Picraux, and J. S. Williams, Materials Research Society Symposia Proceedings No. 74 (Materials Research Society, Pittsburgh, 1987), p. 103.
[35] M. C. Downer, R. L. Fork, and C. V. Shank, J. Opt. Soc. Am. B **2**, 595 (1985).
[36] A. Onuki, Phys. Rev. B **12**, 6740 (1991).
[37] B. S. Luk'yanchuk, N. M. Bytiurin, S. I. Anisimov, N. D. Arnold, and D. Bauerle, in *High Power Laser Ablation*, edited by C. R. Phipps, Proc. SPIE 3343 (in print).

Downloaded 24 Mar 2009 to 134.100.32.208. Redistribution subject to AIP license or copyright; see http://jap.aip.org/jap/copyright.jsp